Journal of
Ceramic Science
and Technology

J. Ceram. Sci. Tech., **08** [01] 67-72 (2017)
DOI: 10.4416/JCST2016-00089
available online at: http://www.ceramic-science.com

Photocatalytic Properties of Nanocrystalline TiO_2 coupled with Up-Conversion Phosphors

S. Mavengere, H. M. Yadav, J.-S. Kim*

Department of Materials Science and Engineering, University of Seoul, Seoul 02504, Republic of Korea
received October 28, 2016; received in revised form December 9, 2016; accepted January 10, 2017

Abstract

$NaYF_4$:(Yb^{3+}, Er^{3+}) up-conversion phosphor was synthesized with the combustion method and coated with TiO_2 nanoparticles by means of a sol-gel technique. Emission peaks of the up-conversion phosphor were located at 523, 544 and 655 nm under irradiation with a 980 nm infrared (IR) dot laser light with 40 mW. TiO_2-coated $NaYF_4$:(Yb^{3+}, Er^{3+}) phosphor showed similar emission peaks with reduced intensities. The photocatalytic activity of the TiO_2-coated up-conversion phosphor particles was investigated based on the degradation of aqueous methylene blue (MB) solution under irradiation with a 200-W visible light of wavelength $\lambda > 410$ nm. TiO_2-coated $NaYF_4$:(Yb^{3+}, Er^{3+}) phosphor particles showed enhanced photocatalytic activity compared with pure TiO_2 powders. The mechanism for enhanced photocatalytic activity was explained in relation to the energy band structure that exists at the interlayer between the $NaYF_4$:(Yb^{3+}, Er^{3+}) phosphor and TiO_2 nanoparticles.

Keywords: Up-conversion phosphor, $NaYF_4$:(Yb^{3+}, Er^{3+}), TiO_2,photocatalysis, visible-light photo-reaction

I. Introduction

TiO_2 is a widely used semiconductor in the synthesis of photocatalysts for environmental pollution control, photovoltaics, sensors, conversion and energy storage devices because of its unique photoelectric properties, high chemical stability and environmental safety. The major drawback of TiO_2 in photocatalysis application is the high charge recombination rate and wide band gap of 3.0 ~ 3.2 eV, which limits electron and hole photogeneration under visible light irradiation. Research has been conducted on TiO_2 photocatalysts to modify them to absorb visible light irradiation. The methods for modifying TiO_2-based photocatalysts consist of metal ion doping of TiO_2 with metals such as Fe, Cr, Ni and Ag [1–3]; and coupling TiO_2 with inorganic oxides such as SiO_2, SnO_2 and WO_3 [4,5]. In addition, long-lasting phosphors have been coupled with TiO_2 photocatalysts to enhance visible light absorption. The TiO_2 photocatalysts coupled with long-lasting phosphor materials such as (Ca,Sr)O-Al_2O_4:Eu^{3+} compounds showed enhanced photocatalytic activity under visible light irradiation [6,7].

One interesting phosphor for coupling with photocatalysts is a kind of up-conversion phosphor since it is capable of absorbing near-infrared (NIR) light. $NaYF_4$ is considered an efficient up-conversion host matrix with low phonon energy and a wide band gap of ~ 8 eV. The crystal structures of $NaYF_4$ exist in two polymorphic forms, which are cubic (α) and hexagonal (β) phases. Up-conversion efficiency depends on the phase and particle size. For example, the β-$NaYF_4$ phase exhibits ~ 10 times higher up-conversion efficiency than α-$NaYF_4$ [8]. $NaYF_4$ co-doped with $Yb^{3+}$and Er^{3+} ions forms up-conversion phosphors with the average particles sizes of 30 – 40 nm, which were synthesized with a combustion method at 650 °C. Low-temperature combustion synthesis of up-conversion phosphors has several advantages over other traditional methods such as a precise stoichiometric ratio, low temperature and short reaction time [9]. Yb^{3+} ions have a large absorption cross-section to 980 nm laser diode excitation source, and therefore it acts as a sensitizer while Er^{3+} ions act as an activator [10]. The up-conversion photoluminescence occurs through energy transfer from Yb^{3+} to Er^{3+}, producing either green, red or blue ultraviolet light when irradiated with NIR photons [11]. Up-conversion emission peak intensities and ratio of various peaks are influenced by the dopant concentration (Yb^{3+}, Er^{3+}), excitation power, preparation temperature and impurities in the starting materials [12].

In this study, the coupling of TiO_2 with up-conversion phosphor $NaYF_4$:(Yb^{3+}, Er^{3+}) was attempted to produce a new photocatalyst composite which could work under ultraviolet (UV), visible and NIR irradiation. The two-step combustion method was adapted for preparing the up-conversion phosphor $NaYF_4$:(Yb^{3+}, Er^{3+}) particles, and then followed by coating of the TiO_2 layer in a sol-gel process. The photocatalytic activities of TiO_2-coated up-conversion phosphor $NaYF_4$:(Yb^{3+}, Er^{3+}) were investigated using the photodegradation of aqueous methylene blue (MB) solution under visible light irradiation.

II. Materials and Methods

(1) Materials

Titanium (IV) n-butoxide, Yb_2O_3 (99.99%) and Er_2O_3 (99.99 %)were purchased from Sigma-Aldrich. HNO_3 (70 %), Na_2SiF_6 (98.0%) and NH_4HF_2 (95.0 %) were purchased from Duksan Chemicals. $CO(NH_2)_2$ (99.0 %)

* Corresponding author: jskim@uos.ac.kr

and Y_2O_3 (99.99 %) were procured from Samchun Chemicals and Daejung Chemicals, respectively. All chemicals were used as-received and all experiments were performed in deionized water.

(2) Synthesis of phosphor and TiO_2-coated phosphor

Up-conversion phosphor samples were prepared with a simple solution combustion method. In a typical synthesis, the oxide powders of Y_2O_3 (99.99 %), Yb_2O_3 (99.99 %) and Er_2O_3 (99.99 %) in a molar ratio of 0.90: 0.09: 0.01 were dissolved in HNO_3 (70 %) under vigorous stirring at 120 °Cto form an oxide solution. Simultaneously, another aqueous solution of Na_2SiF_6 (98.0 %), and NH_4HF_2 (95.0 %) was prepared on a hot plate under magnetic stirring at 80 °C. The two solutions were mixed on a magnetic stirring hot plate followed by addition of $CO(NH_2)_2$ (99.0 %) as fuel at 70 °C for 2 h. Then, the obtained solution was placed in a closed crucible for combustion reaction at 650 °C for 5 minutes in a muffle furnace at a heating rate of 5 °C/min. The up-conversion phosphor powders were further annealed for 2 h at 580 °C.

The $NaYF_4$:(Yb^{3+}, Er^{3+}) phosphor powders were coated with TiO_2 by means of a sol-gel processing technique. The samples for investigating the photocatalytic activity of TiO_2-coated $NaYF_4$:(Yb^{3+}, Er^{3+}) phosphor were prepared using various concentrations of titanium (IV) n-butoxide (TBOT). The concentrations ranging from 0.064 M to 0.632 M TBOT, 50 ml ethanol and 10 ml water were mixed and stirred magnetically at 50 °C for 2 h to obtain TiO_2 sol. Then, the $NaYF_4$:(Yb^{3+}, Er^{3+}) phosphor powders were dispersed in the TiO_2 sol under magnetic stirring for 30 minutes to allow uniform coating, filtered and washed with de-ionized water. The TiO_2-coated $NaYF_4$:(Yb^{3+}, Er^{3+}) phosphor particles were dried in an electric oven at 100 °C for 12 h and annealed in an electric furnace at a heating rate of 5 °C/min for 1 h at 450 °C.

(3) Characterization

X-ray diffraction (XRD) patterns were obtained on a Bruker D8-Advance diffractometer using Cu-Kα radiation at 2θ ranges from 10° to 80°. Field emission scanning electron microscopy (FE-SEM, FEI Nova Nano SEM 200) was used to observe the morphology of the up-conversion phosphor particles. Transmission electron microscopy (TEM, FEI Technai F20 G^2) was used to observe the surface morphology of TiO_2-coated $NaYF_4$:(Yb^{3+}, Er^{3+}) phosphor samples. The up-conversion photoluminescence (PL) spectra was analyzed on a fluorescence spectrophotometer (F-4500, Hitachi) operating at 400 V, with excitation slit of 1 nm and emission slit of 10 nm. For PL measurement, 200 mg of photocatalyst powders were placed in a sample holder and irradiated using a 40 mW IR dot laser lamp of 980 nm (Laserlab). The excitation wavelength was fixed at 980 nm for all photocatalyst samples. An UV-Vis spectrophotometer (UV-1601, Shimadzu) was used to measure the absorption spectrum of MB solutions after visible light irradiation with TiO_2-coated $NaYF_4$:(Yb^{3+}, Er^{3+}) phosphor samples.

(4) Photocatalytic experiments

The photocatalytic activity was investigated by measuring the photodegradation of an aqueous MB solution under visible light irradiation. The maximum absorbance of MB solution was observed at 664 nm with the range of 1.00 ~ 1.20. Nanocrystalline TiO_2-coated $NaYF_4$:(Yb^{3+}, Er^{3+}) phosphor powders (700 mg) were dispersed in 100 mL 5-ppm-MB solution and irradiated with a visible light lamp (200 W clear/soft tone, IL Kwang Co., Ltd. Korea). Photocatalyst powders were in suspension under magnetic stirring at 300 rpm throughout the experiment. The photocatalyst samples dispersed in MB solution were placed in darkness for 30 minutes under magnetic stirring to reach chemical equilibrium before irradiation with visible light. An UV-light cut-off lens (Kenko zeta UV L41, Japan) was inserted below the visible light lamp to filter ultraviolet wavelengths below 410 nm. At 1-hour intervals, 1 mL solution was pipetted from the reaction mixture. The samples were centrifuged and placed in quartz cuvettes for absorption measurements.

III. Results and Discussion

(1) Characterization of TiO_2-coated phosphor

Fig. 1(a) shows XRD patterns for two samples of TiO_2-coated $NaYF_4$:(Yb^{3+}, Er^{3+}) phosphor particles (coated with 0.106 M TBOT and annealed at 450 or 750 °C), $NaYF_4$:(Yb^{3+}, Er^{3+}) phosphor and pure TiO_2 (prepared from 0.106 M TBOT precursor). Fig. 1(b) shows enlarged XRD patterns of Fig. 1(a) from 10° to 30° of 2θ. The peaks in the pure $NaYF_4$:(Yb^{3+}, Er^{3+}) phosphor correspond well with cubic phase $NaYF_4$ (JCPDS 04 – 008 – 3253) and the peaks in the TiO_2 to anatase phase (JCPDS 04 – 006 – 9240). The TiO_2 anatase peak at 24.5° was observed in the TiO_2-coated $NaYF_4$:(Yb^{3+}, Er^{3+}) phosphor and its intensity increased with increasing annealing temperature from 450 to 750 °C. In the TiO_2-coated $NaYF_4$:(Yb^{3+}, Er^{3+}) phosphor heat-treated at 750 °C, peak suppression occurred at 16° and 22.5°, whilst new peaks appeared at 12° and 14.2°. TiO_2 rutile phase at 27.5° is observed at 750 °C due to anatase transformation. The peaks at 12° and 14.2° for the sample at 750 °C can be assigned to $Na_2Ti_6O_{13}$ intermetallic compound which is formed at temperatures above 700 °C [13].

Fig. 2(a) shows an FE-SEM image of $NaYF_4$:(Yb^{3+}, Er^{3+}) phosphor. The sample consists of clusters of regular polygon-shaped particles with average size of 100 nm. Fig. 2(b) shows an FE-SEM image of TiO_2-coated $NaYF_4$:(Yb^{3+}, Er^{3+}). Nanocrystalline TiO_2 particles are formed as coating layers or in clusters around the $NaYF_4$:(Yb^{3+}, Er^{3+}) particles.

Fig. 3(a) shows the TEM image of TiO_2-coated $NaYF_4$:(Yb^{3+}, Er^{3+}) up-conversion phosphor particles. The image shows two distinct morphologies, small particles of 10 nm and large polygonal-like particles of about 100 nm. Energy-dispersive spectroscopy (EDS) confirmed that the bright-contrast small particles are TiO_2. The dark-contrast large particles were confirmed to be $NaYF_4$:(Yb^{3+}, Er^{3+}) phosphor. Fig. 3(b) shows EDS spectra obtained from the edge of $NaYF_4$:(Yb^{3+}, Er^{3+}) phosphor material while the EDS spectra of a TiO_2 particle are shown in Fig. 3(c). The EDS analysis shows the presence of sodium (Na), fluorine (F), oxygen (O), ytterbium (Yb), erbium (Er) and titanium (Ti) peaks, confirming the presence of $NaYF_4$:(Yb^{3+}, Er^{3+}) and TiO_2.

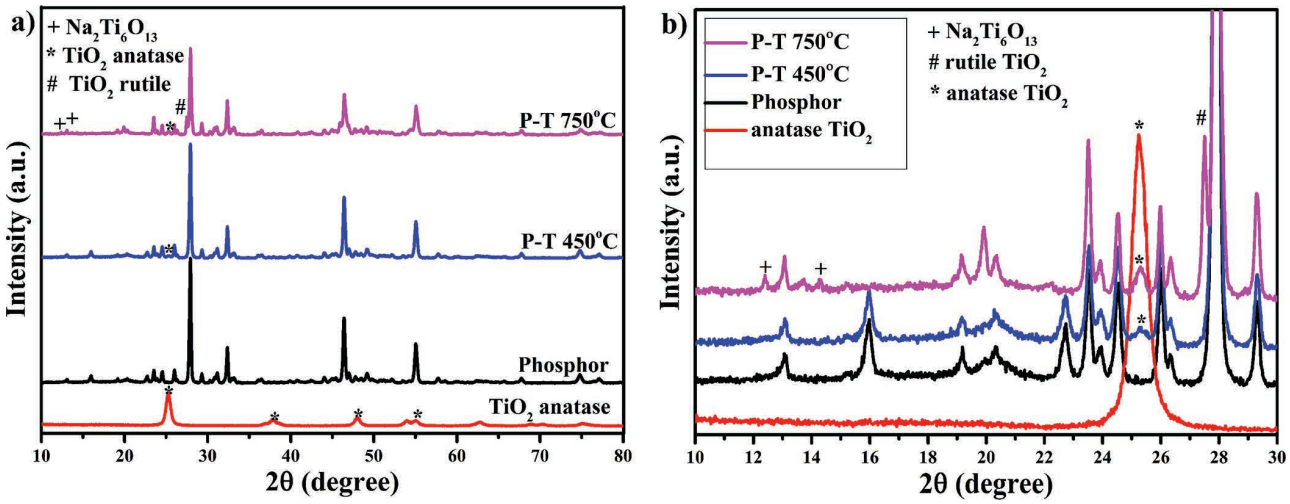

Fig. 1: (a) XRD patterns of $NaYF_4$:(Yb^{3+}, Er^{3+})/TiO_2 (P-T), phosphor $NaYF_4$:(Yb^{3+}, Er^{3+}) and pure TiO_2. (b) Enlarged XRD patterns of the samples in the range of 10–30° of 2θ.

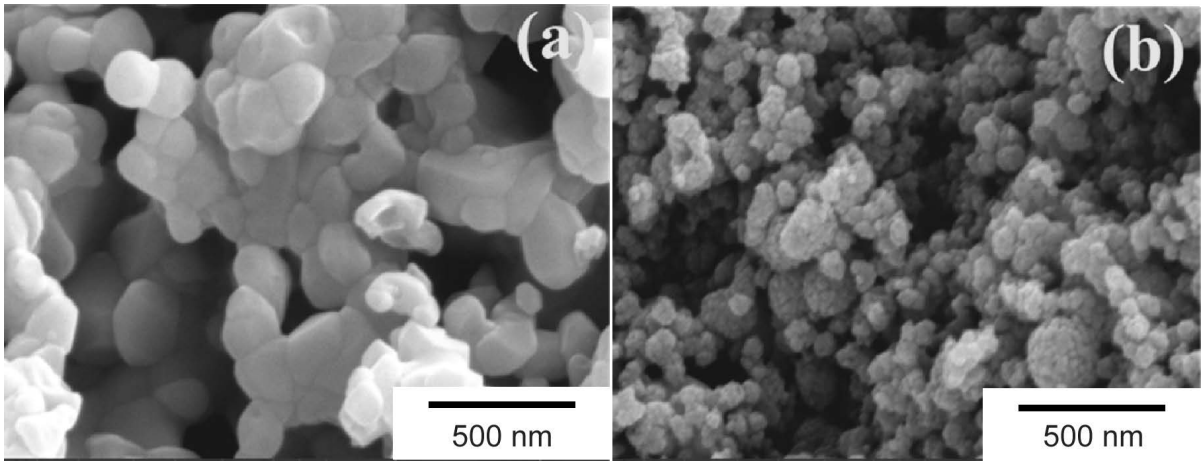

Fig. 2: FE-SEM images of (a) $NaYF_4$:(Yb^{3+}, Er^{3+}) and (b) TiO_2-coated $NaYF_4$:(Yb^{3+}, Er^{3+}) phosphor.

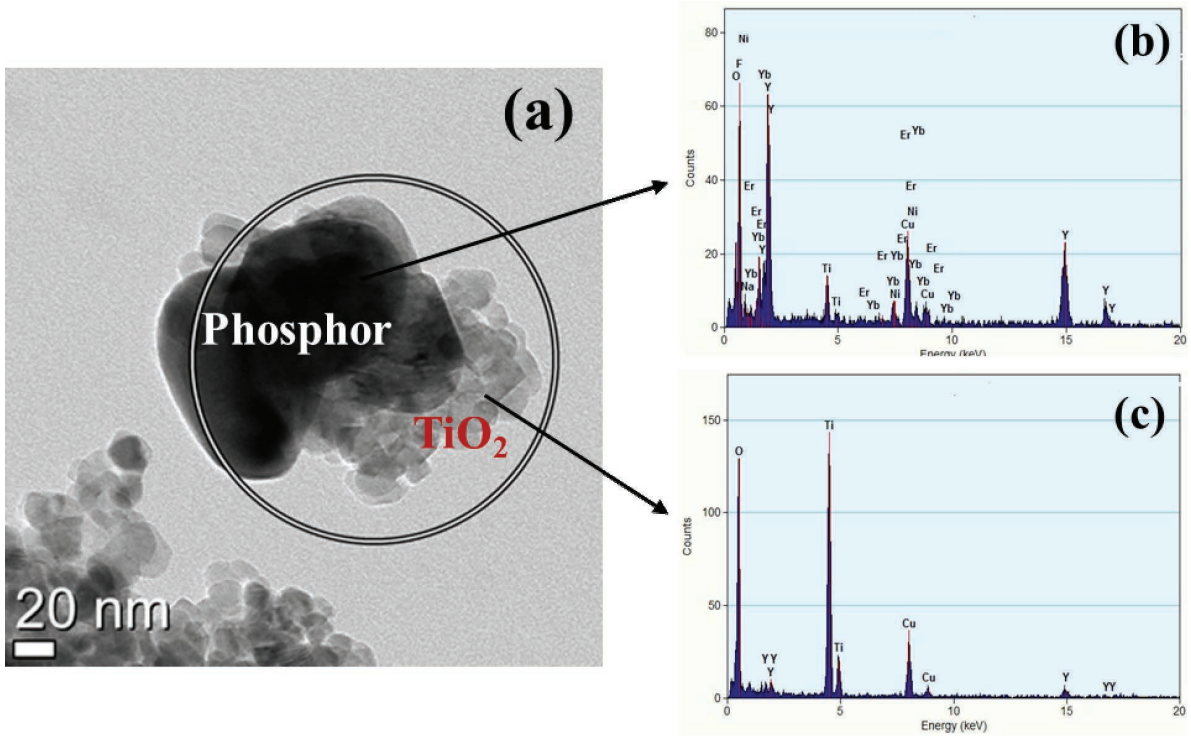

Fig. 3: (a) TEM image of TiO_2-coated $NaYF_4$:(Yb^{3+}, Er^{3+}) phosphor and (b-c) corresponding EDS spectra.

Fig. 4 shows photoluminescence spectra of TiO_2-coated $NaYF_4$:(Yb^{3+}, Er^{3+}) phosphor with different concentrations of TBOT. The spectra for the $NaYF_4$:(Yb^{3+}, Er^{3+}) phosphor were superimposed with those of the TiO_2-coated $NaYF_4$:(Yb^{3+},Er^{3+}), which are labelled with respective TBOT coating concentration. The distinct emission peaks are located at 523, 544 and 655 nm. These results also correspond to the findings of other researchers; where 523 and 544 nm peaks are assigned to Er^{3+} transition from $^2H_{11/2}$ and $^4S_{3/2}$ to $^4I_{15/2}$ respectively and 655 nm is assigned to $^4F_{9/2}$ to $^4I_{15/2}$ transition [8]. The luminescence spectra for sol-gel TiO_2-coated $NaYF_4$:(Yb^{3+}, Er^{3+}) powder show similar peak positions at 523, 544 and 655 nm but with reduced emission intensities. The TiO_2 coating on up-conversion phosphor tends to act as a barrier to excitation and emission of phosphor, thus the intensity of photoluminescence emission peaks decreased with the increasing concentration of TBOT above 0.106 M.

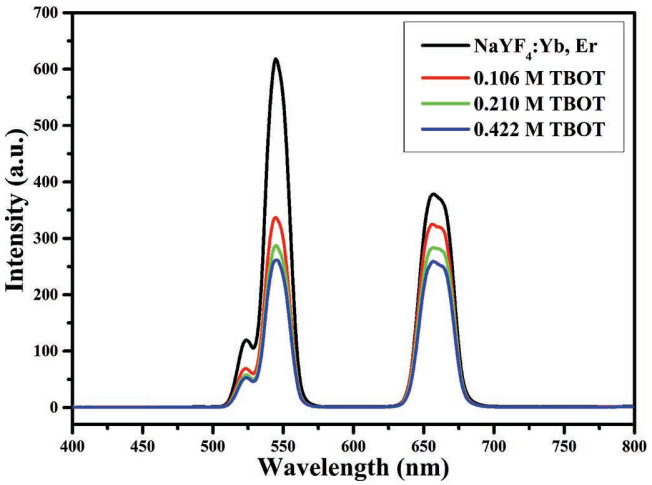

Fig. 4: Up-conversion photoluminescence spectra of $NaYF_4$:(Yb^{3+}, Er^{3+}) with different concentrations of TBOT.

(2) Photocatalytic activity of TiO_2-coated phosphor

Fig. 5 shows the absorbance spectra of the MB solution mixed with TiO_2 coated $NaYF_4$:(Yb^{3+}, Er^{3+}) phosphor powders with 0.106 M TBOT under visible-light irradiation for 14 h. The photodegradation of the MB solution was observed through reduction in absorbance peak intensities at 664 nm with irradiation time. This decrease in the absorption peak intensities at 664 nm was used to assess the photocatalytic activity. Fig. 6 shows variations of maximum absorbance intensities for MB solutions sensitized using TiO_2-coated $NaYF_4$:(Yb^{3+}, Er^{3+}) under visible-light irradiation as irradiation time. Different TiO_2 coatings on phosphor were achieved by varying the concentration of TBOT. The data obtained from pure $NaYF_4$:(Yb^{3+}, Er^{3+}) phosphor and TiO_2 samples were superimposed for comparison in the photocatalytic activity. The absorbance peaks for pure phosphor $NaYF_4$:(Yb^{3+}, Er^{3+}) and TiO_2 samples remained constant, showing that no photodegradation of the aqueous MB solution occurred during irradiation with visible light. The decrease in absorbance of aqueous MB solution with irradiation time indicates the progression of MB photocatalytic activity in TiO_2 coated $NaYF_4$:(Yb^{3+}, Er^{3+}) phosphor powders. This photocatalytic reaction in TiO_2-coated $NaYF_4$:(Yb^{3+},Er^{3+}) phosphor with visible-light irradiation is attributed to free sodium ions which diffuse from the $NaYF_4$:(Yb^{3+},Er^{3+}) phosphor matrix to the TiO_2 layer along the interface of phosphor to form sodium titanate intermetallic compound, of the general formula $Na_2Ti_{2n}O_{2n+1}$ with an absorption band (~2.81 eV) in the visible light region [14]. A similar visible-light photocatalytic reaction was observed with TiO_2-coated (Ca,Sr)O-Al_2O_3:Eu^{3+} phosphor composites in which the intermetallic compounds of (Ca,Sr)TiO_3 were formed at the interface between phosphors and TiO_2 [6, 15].

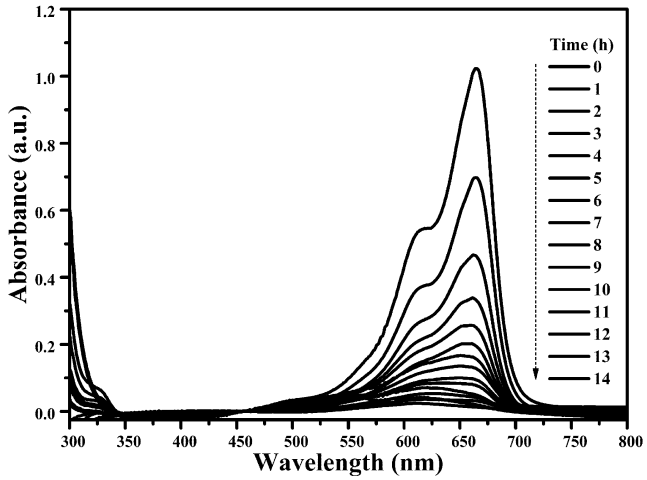

Fig. 5: Absorbance spectra of the MB solution for TiO_2-coated NaYF4:(Yb3+, Er3+) with 0.106 M TBOT under visible light irradiation.

The variation of MB absorbance peaks with TBOT concentration in $NaYF_4$:(Yb^{3+}, Er^{3+}) phosphor samples was attributed to the different coating thickness of the TiO_2 layer. It was found that a sufficient TiO_2 coating layer would permit photo-excitation of the TiO_2-coated phosphor composites to produce enough electron-hole pairs for photodegradation of the MB dye solutions. Therefore, 0.106 M TBOT coating on $NaYF_4$:(Yb^{3+}, Er^{3+}) phosphor was the appropriate TBOT concentration for fast MB photodegradation as shown in Fig. 6. On the other hand, excessively thick TiO_2 coatings may cause the photo-excitation of TiO_2-coated phosphors to decrease by hindering the light absorption of phosphors. Hence, 0.422 M TBOT coating resulted in lower photocatalytic activity due to blocking of light by TiO_2 particles, resulting in low photoluminescence intensity of this sample in Fig. 4.

(3) Photocatalytic mechanism of TiO_2-coated phosphor

The possible energy band structure for the $NaYF_4$:(Yb^{3+}, Er^{3+}); $Na_2Ti_{2n}O_{2n+1}$ and TiO_2 is shown in the schematic diagram in Fig. 7. However, the role of $NaYF_4$:(Yb^{3+}, Er^{3+}) phosphor particles is to offer a stable crystalline support for the TiO_2 photocatalyst and provides photoluminescence. In addition to that, the $NaYF_4$:(Yb^{3+}, Er^{3+}) phosphor particles are a source of Na^+ ions, which diffuse to form intermetallic compound sodium titanate during crystallization of TiO_2 coating. This sodium titanate at the interface of the $NaYF_4$:(Yb^{3+}, Er^{3+}) phosphor particle and TiO_2 coating is thought to be photoreactive to visible light. In addition to that, differ-

ent fermi levels in $NaYF_4$:(Yb^{3+}, Er^{3+}) phosphor, intermetallic compound $Na_2Ti_{2n}O_{2n+1}$ and TiO_2 might have induced energy band bending at the junction and extend the absorption band of TiO_2 towards the visible light region. Thus, light photons emitted from the phosphors, promote the photo-generation of electron-hole pairs in TiO_2-coated $NaYF_4$:(Yb^{3+}, Er^{3+}) phosphor through intermetallic compound and enhance the photocatalytic activity of TiO_2 even under visible light irradiation.

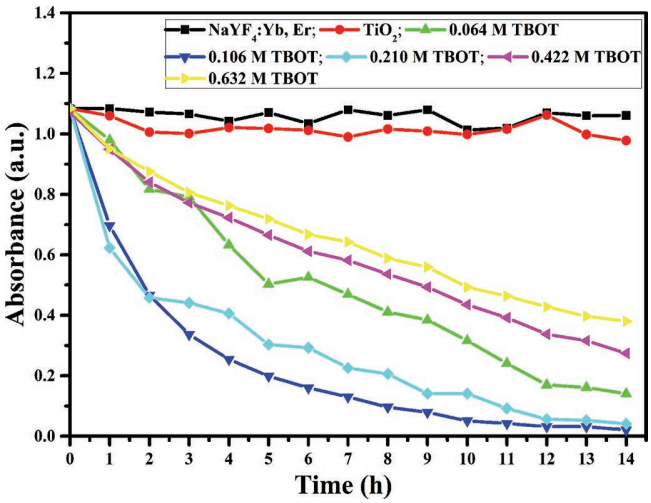

Fig. 6: Variation of absorbance spectra for the MB solution with TiO2-coated NaYF4:(Yb3+, Er3+) phosphor under visible light irradiation.

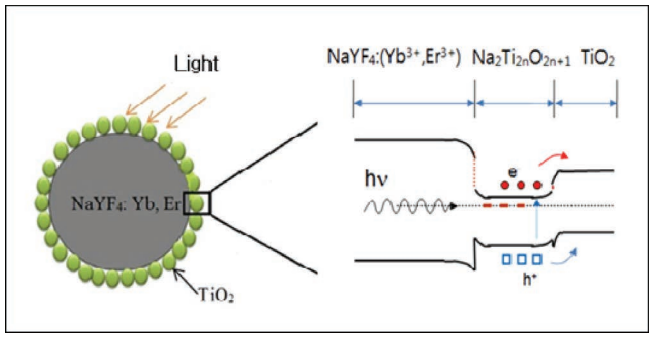

Fig. 7: Schematic energy band structure at the interfaces of $NaYF_4$:(Yb^{3+}, Er^{3+}), $Na_2Ti_{2n}O_{2n+1}$ and TiO_2.

IV. Conclusions

TiO_2-coated $NaYF_4$:(Yb^{3+}, Er^{3+}) phosphor synthesized with a simple solution combustion and sol-gel method. TiO_2-coated $NaYF_4$:(Yb^{3+}, Er^{3+}) phosphor materials were capable of the photodegradation of aqueous methylene blue (MB) solutions under visible light irradiation. The highest MB photodegradation occurred for the TiO_2-coated $NaYF_4$:(Yb^{3+}, Er^{3+}) phosphor (coated with 0.106 M titanium (IV) n-butoxide (TBOT)). The visible-light photocatalytic reaction of TiO_2-coated $NaYF_4$:(Yb^{3+}, Er^{3+}) phosphor may result in the formation of intermetallic compound, $Na_2Ti_{2n}O_{2n+1}$, which induces TiO_2 to be photo-reactive under visible-light irradiation. The visible-light photocatalysis of TiO_2-coated up-conversion phosphor is plausibly applicable for environmental remediation.

Acknowledgements

This work was supported by the 2016 Research Fund of the University of Seoul.

References

1 Yadav, H.M., Kolekar, T.V, Pawar, S.H., Kim, J.-S.: Enhanced photocatalytic inactivation of bacteria on Fe-containing TiO_2 nanoparticles under fluorescent light, *J. Mater. Sci. Mater. Med.*, **27**, 57, (2016).

2 Yadav, H.M. *et al.*: Enhanced visible light photocatalytic activity of Cr^{3+}-doped anatase TiO_2 nanoparticles synthesized by sol-gel method, *J. Mater. Sci. Mater. Electron.*, **27**, 526 – 534, (2015).

3 Lin, W., Cheng, H., Ming, J., Yu, Y., Zhao, F.: Deactivation of Ni/TiO_2 catalyst in the hydrogenation of nitrobenzene in water and improvement in its stability by coating a layer of hydrophobic carbon, *J. Catal.*, **291**, 149 – 154, (2012).

4 Lafond, V., Mutin, P.H., Vioux, A.: Non-hydrolytic sol-gel routes based on alkyl halide elimination: toward better mixed oxide catalysts and new supports application to the preparation of a SiO_2-TiO_2 epoxidation catalyst, *J. Mol. Catal. A: Chem.*, **182 – 183**, 81 – 88, (2002).

5 Pan, J.H., Sun, D.D., Lee, W.I.: Preparation of periodically organized mesoporous bicomponent TiO_2 and SnO_2-based thin films by controlling the hydrolytic kinetics of inorganic precursors during EISA process, *Mater. Lett.*, **65**, 2836 – 2840, (2011).

6 Kim, J.S., Sung, H.J., Kim, B.J.: Photocatalytic characteristics for the nanocrystalline TiO_2 on the Ag-doped $CaAl_2O_4$:(Eu,Nd) phosphor, *Appl. Surf. Sci.*, **334**, 151 – 156, (2015).

7 Kim, J.-S., Kim, S.-W., Jung, S.-C.: Photocatalytic reaction characteristics of the titanium dioxide supported on the long phosphorescent phosphor by a low pressure chemical vapor deposition, *J. Nanosci. Nanotechnol.*, **14**, 7751 – 7755, (2014).

8 Chen, D. *et al.*: Dopant-induced phase transition: A new strategy of synthesizing hexagonal upconversion $NaYF_4$ at low temperature, *Chem. Commun. (Camb).*, **47**, 5801 – 5803, (2011).

9 Tamrakar, R.K., Bisen, D.P., Upadhyay, K., Sahu, I.P.: Upconversion and colour tunability of Gd_2O_3:Er^{3+} phosphor prepared by combustion synthesis method, *J. Alloy. Compd.*, **655**, 423 – 432, (2016).

10 Gonell, F. *et al.*: Photon up-conversion with lanthanide doped oxide particles for solar H_2 generation, *J. Phys. Chem. C*, **118**, 140505212111008, (2014).

11 Liu, Y. *et al.*: Coupling effects of Au-decorated core-shell β-$NaYF_4$:Er/Yb@SiO_2 microprisms in dye-sensitized solar cells: plasmon resonance versus upconversion, *Electrochim. Acta*, **180**, 394 – 400, (2015).

12 Bednarkiewicz, A., Wawrzynczyk, D., Nyk, M., Samoć, M.: Tuning red-green-white up-conversion color in nano $NaYF_4$:Er/Yb phosphor, *J. Rare Earth.*, **29**, 1152 – 1156, (2011).

13 Sauvet, A.-L., Baliteau, S., Lopez, C., Fabry, P.: Synthesis and characterization of sodium titanates $Na_2Ti_3O_7$ and $Na_2Ti_6O_{13}$, *J. Solid State Chem.*, **177**, 4508 – 4515, (2004).

14 Bavykin, D.V., Walsh, F.C.: Kinetics of alkali metal ion exchange into nanotubular and nanofibrous titanates, *J. Phys. Chem. C*, **111**, 14644 – 14651, (2007).

15 Yoon, J.-H., Kim, J.-S.: Investigation of photocatalytic reaction for the titanium dioxide-phosphor composite, *Ionics (Kiel)*, **16**, 131 – 135, (2010).